CHIN. PHYS. LETT. Vol. 37, No. 3 (2020) 038504

Effect of Lattice Distortion on the Magnetic Tunnel Junctions Consisting of Periodic Grating Barrier and Half-Metallic Electrodes *

He-Nan Fang(方贺男)[1**], Yuan-Yuan Zhong(仲元园)[1], Ming-Wen Xiao(肖明文)[2], Xuan Zang(臧璇)[1], Zhi-Kuo Tao(陶志阔)[1]

[1]*College of Electronic and Optical Engineering, Nanjing University of Posts and Telecommunications, Nanjing 210023*
[2]*Department of Physics, Nanjing University, Nanjing 210093*

(Received 8 October 2019)

A spintronic theory is developed to study the effect of lattice distortion on the magnetic tunnel junctions (MTJs) consisting of single-crystal barrier and half-metallic electrodes. In the theory, the lattice distortion is described by strain, defect concentration and recovery temperature. All three parameters will modify the periodic scattering potential, and further alter the tunneling magnetoresistance (TMR). The theoretical results show that: (1) the TMR oscillates with all the three parameters; (2) the strain can change the TMR about 30%; (3) the defect concentration will strongly modify the periodic scattering potential, and further change the TMR about 50%; and (4) the recovery temperature has little effect on the periodic scattering potential, and only can change the TMR about 10%. The present work may provide a theoretical foundation to the application of lattice distortion for MTJs consisting of single-crystal barrier and half-metallic electrodes.

PACS: 85.75.−d, 73.40.Gk, 72.25.−b DOI: 10.1088/0256-307X/37/3/038504

Magnetic tunnel junctions (MTJs) have a great potential in applications, and thus are important research object of spintronics.[1] The barriers of conventional Al–O-based junctions are amorphous, and therefore the effect of disorder scattering in the barriers will lead to a suppressed tunneling magnetoresistance (TMR). As a result, the conventional Al–O-based magnetic tunnel junctions cannot satisfy the requirements of next-generation devices. On the contrary, the barriers of MgO-based magnetic tunnel junctions are single crystals, so a much higher TMR can be achieved compared with Al–O-based junctions.[2,3] For this reason, MgO-based magnetic tunnel junctions have become the research focus of the theory, experiment and applications.[4−8] Apart from the barriers, the electrodes are also important for MTJs to exhibit high TMR. In particular, half-metallic electrodes, whose spin polarization is 100%, will lead to nearly infinite TMR at low temperature and bias in conventional theories.[9] So far, great efforts have been made to research of the MTJs consisting of single-crystal MgO barrier and half-metallic electrodes.[10−15] In the course of experimental study, many novel physical phenomena have been found in this kind of MTJs. Among them, the temperature dependence of TMR is widely investigated.[12,16,17] It is found that the parallel resistance ($R_{\rm P}$)[12] or TMR[16,17] can oscillate with temperature, which is quite different from the MTJs with normal (not half-metallic) electrodes. This intriguing phenomenon is also observed in MTJs consisting of Ag barrier and half-metallic electrodes.[18] Certainly, the physical mechanism for this phenomenon needs to be studied theoretically.

Previously, we theoretically studied the temperature dependence of parallel resistance, antiparallel resistance ($R_{\rm AP}$) and TMR in MgO-based MTJs with normal electrodes.[19] It was found that the effect of the lattice distortion can be account for the temperature dependence. To be specific, the effect of the lattice distortion of the barrier can be described by strain, defect concentration, and recovery temperature. These three physical quantities all influence the temperature dependence through the modification of the scattering potential of the barrier. In this Letter, we try to extend the previous theory to deal with the temperature dependence in MTJs consisting of single-crystal barrier and half-metallic electrodes.

To begin with, we employ a perfect periodic potential $U(\boldsymbol{r})$ to describe the single-crystal barrier of the MTJs. It can be written as

$$U(\boldsymbol{r}) = \sum_{l_3=0}^{n-1} \sum_{\boldsymbol{R}_{\rm h}} v(\boldsymbol{r} - \boldsymbol{R}_{\rm h} - l_3\boldsymbol{a}_3), \tag{1}$$

where $v(\boldsymbol{r})$ is the single atomic potential of the barrier; n represents the total number of the layers of the barrier; $\boldsymbol{R}_{\rm h} = l_1\boldsymbol{a}_1 + l_2\boldsymbol{a}_2$, with $\boldsymbol{a}_1$ and $\boldsymbol{a}_2$ being the intralayer primitive vectors of barrier, and l_1 and l_2 the corresponding integers; $\boldsymbol{a}_3$ is the interlayer primitive vector of the barrier, with l_3 the corresponding integer.

Let the z-axis be antiparallel to the tunneling current. The transmission coefficient for the channel of the spin-up to spin-up tunneling can be written

*Supported by the National Natural Science Foundation of China under Grant Nos. 11704197 and 61574079, and the NUPTSF under Grant No. NY217046.
**Corresponding author. Email: fanghn@njupt.edu.cn
© 2020 Chinese Physical Society and IOP Publishing Ltd

as[19,20]

$$T_{\uparrow\uparrow}(\boldsymbol{k}) = \frac{1}{8k_z}\left[p_+^z e^{i[p_+^z-(p_+^z)^*]d} + p_-^z e^{i[p_-^z-(p_-^z)^*]d} + q_+^z e^{i[q_+^z-(q_+^z)^*]d} + q_-^z e^{i[q_-^z-(q_-^z)^*]d} + [p_+^z e^{i[p_+^z-(p_-^z)^*]d} + p_-^z e^{i[p_-^z-(p_+^z)^*]d} - q_+^z e^{i[q_+^z-(q_-^z)^*]d} - q_-^z e^{i[q_-^z-(q_+^z)^*]d}] + \text{c.c.}\right], \tag{2}$$

where k denotes the incident wave vector of tunneling electrons, and k_z is its z-component, d represents the thickness of barrier, and

$$p_\pm^z = \left[\boldsymbol{k}^2 - \boldsymbol{k}_\text{h}^2 \pm 2m\hbar^{-2}v\left(\boldsymbol{K}_\text{h}\right)\right]^{1/2}, \tag{3a}$$

$$q_\pm^z = \left[\boldsymbol{k}^2 - \left(\boldsymbol{k}_\text{h}+\boldsymbol{K}_\text{h}\right)^2 \pm 2m\hbar^{-2}v\left(\boldsymbol{K}_\text{h}\right)\right]^{1/2}. \tag{3b}$$

Here k_h is the intralayer component of k, K_h is the intralayer reciprocal lattice vector, and $v\left(\boldsymbol{K}_\text{h}\right)$ is the Fourier transformation of $v\left(\boldsymbol{r}\right)$. From $T_{\uparrow\uparrow}$, the conductance $G_{\uparrow\uparrow}$ can be expressed as

$$G_{\uparrow\uparrow} = \frac{e^2}{16\pi^3\hbar}\int_0^{\pi/2} d\theta \int_0^{2\pi} d\phi k_{\text{F}\uparrow}^2 \sin\left(2\theta\right) T_{\uparrow\uparrow}\left(k_{\text{F}\uparrow},\theta,\phi\right), \tag{4}$$

where e denotes the electron charge, θ the angle between k and e_z, ϕ the angle between k_h and a_1, and $k_{\text{F}\uparrow}$ the Fermi wave vector of the spin-up electrons. Similarly, $G_{\uparrow\downarrow}$, $G_{\downarrow\uparrow}$, and $G_{\downarrow\downarrow}$ can be obtained. As usual, $G_\text{P} = G_{\uparrow\uparrow} + G_{\downarrow\downarrow}$, $G_\text{AP} = G_{\uparrow\downarrow} + G_{\downarrow\uparrow}$, $R_\text{P} = 1/G_\text{P}$, $R_\text{AP} = 1/G_\text{AP}$ and $\text{TMR} = G_\text{P}/G_\text{AP} - 1 = R_\text{AP}/R_\text{P} - 1$.

It is worth noting that, for the MTJs with half-metallic electrodes, there are no spin-down electrons; i.e., $G_{\uparrow\downarrow} = G_{\downarrow\downarrow} = 0$. In the conventional theories, the conductance $G_{\uparrow\downarrow}$ is also equal to zero due to the energy conservation, which means that $G_\text{AP} = 0$ and $\text{TMR} = +\infty$. However, in the present theory, the energy of the tunneling electron can be non-conserved according to the Bethe theory and two-beam approximation,[19–21] which has been discussed in detail in Ref. [22]. Therefore, the incident electrons will possess enough energy to transit into the spin-down band of the lower electrode when $v\left(\boldsymbol{K}_\text{h}\right) > \Delta - \mu$. This leads to $G_\text{AP} = G_{\uparrow\downarrow} \neq 0$. As a result, the TMR can be finite if $v\left(\boldsymbol{K}_\text{h}\right) > \Delta - \mu$, and the physical picture has been sketched diagrammatically in Fig. 1. It can explain the problem why the experimental TMR has still been far away from infinity even both electrodes are half-metallic. In the following, we only discuss the case of $v\left(\boldsymbol{K}_\text{h}\right) > \Delta - \mu$, because otherwise the TMR will be infinite as stated in Ref. [22].

As pointed out in Ref. [19], the periodic potential $U\left(\boldsymbol{r}\right)$ will be modified by the lattice distortion. Through the Patterson function approach, the distortion brings the modification of the Fourier transform $v\left(\boldsymbol{K}_\text{h}\right)$ of the atomic potential as follows:

$$v\left(\boldsymbol{K}_\text{h}\right) = \left[1 + 2\frac{\sigma}{1-\sigma}\cos\left(\boldsymbol{K}_\text{h}\cdot\alpha_0\left(1-\frac{T}{T_\text{C}}\right)\right)\right] \cdot (1-\sigma)\, v_0\left(\boldsymbol{K}_\text{h}\right), \tag{5}$$

where σ is the defect concentration, α_0 is the strain of the barrier at zero temperature, T_C is the recovery temperature above which the strain disappears, and $v_0\left(\boldsymbol{K}_\text{h}\right)$ is the Fourier transform of the atomic potential of ideal perfect barrier. Equation (5) builds the relationship of $v\left(\boldsymbol{K}_\text{h}\right)$ and the lattice distortion. The modification of $v\left(\boldsymbol{K}_\text{h}\right)$ by the lattice distortion will then alter the conductances and TMR according to Eqs. (2)–(4).

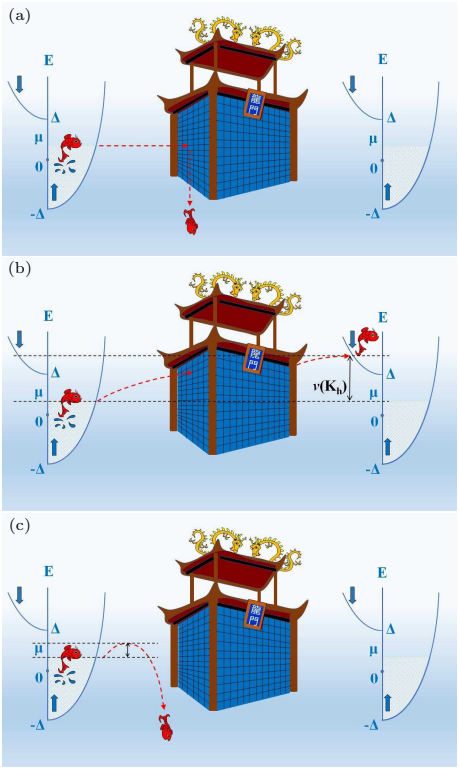

Fig. 1. The diagrammatic pictures for MTJs consisting of single-crystal barrier and half-metallic electrodes: (a) in the conventional theories, $G_\text{AP} = 0$ and $\text{TMR} = +\infty$, (b) in the present theory, if $v\left(\boldsymbol{K}_\text{h}\right) > \Delta - \mu$, $G_\text{AP} \neq 0$ and TMR is finite, (c) in the present theory, if $v\left(\boldsymbol{K}_\text{h}\right) < \Delta - \mu$, $G_\text{AP} = 0$ and $\text{TMR} = +\infty$. The carp represents a tunneling electron, and the "dragon gate" represents a single-crystal barrier.

Next, we display and discuss the calculation results. The parameters of the half-metallic electrodes are set as follows: the chemical potential μ is 7 eV, and the half of the exchange splitting Δ is 12 eV. The parameters of the barrier are set as follows: $K_\text{h} = 2.116 \times 10^{10}\,\text{m}^{-1}$, and $v_0\left(\boldsymbol{K}_\text{h}\right) = 15.3\,\text{eV}$.

As the foundation of the latter studies, we would like to investigate the dependences of R_P and R_AP on $v\left(\boldsymbol{K}_\text{h}\right)$. The results are shown in Fig. 2, where the thickness of the barrier varies from 1.5 nm to 3 nm. It can be seen from Fig. 2 that the R_P oscillates with

$v(\boldsymbol{K}_{\rm h})$, which comes from the inference among the diffracted waves as pointed out in Ref. [19]. However, the $R_{\rm AP}$ does not oscillate with $v(\boldsymbol{K}_{\rm h})$, which is different from the case in Ref. [19]. This is because that p_-^z and q_-^z will always be imaginary for $G_{\uparrow\downarrow}$ due to $\mu < \Delta$. These results suggest that both the $R_{\rm P}$ and $R_{\rm AP}$ can be regulated by $v(\boldsymbol{K}_{\rm h})$. According to Eq. (5), the lattice distortion and temperature will modify $v(\boldsymbol{K}_{\rm h})$, and further alter $R_{\rm P}$ and $R_{\rm AP}$. This is just the physical mechanism for the effect of lattice distortion on TMR. At present, only $R_{\rm P}$ and TMR can oscillate with $v(\boldsymbol{K}_{\rm h})$, and thus oscillate with temperature. This can explain the intriguing phenomenon stated in the introduction.

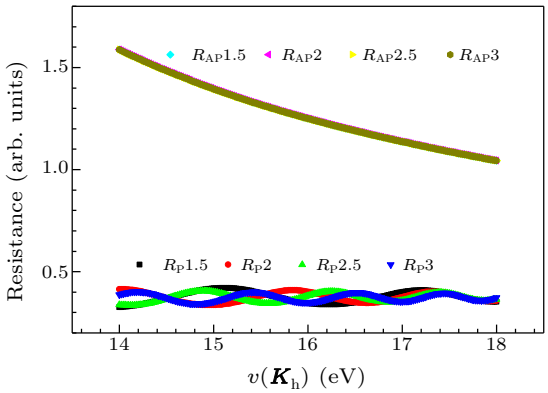

Fig. 2. $R_{\rm P}$ and $R_{\rm AP}$ versus $v(\boldsymbol{K}_{\rm h})$ under different barrier thicknesses $d = 1.5$, 2, 2.5 and 3 nm.

Now, we discuss the effect of the defect concentration, the strain and the recovery temperature on the MTJs.

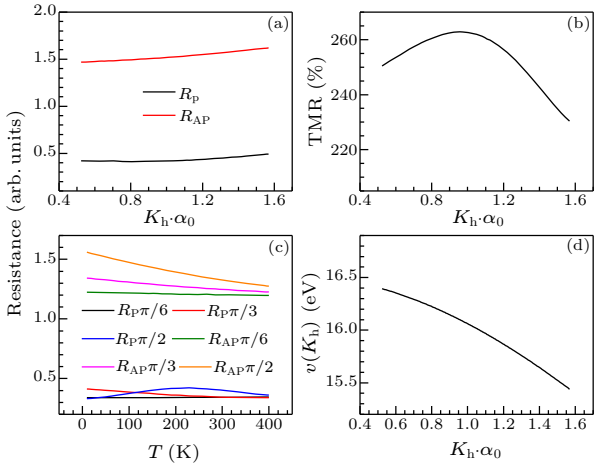

Fig. 3. (a) $R_{\rm P}$ and $R_{\rm AP}$ versus $\boldsymbol{K}_{\rm h}\cdot\alpha_0$ at 300 K, (b) TMR versus $\boldsymbol{K}_{\rm h}\cdot\alpha_0$ at 300 K, (c) $R_{\rm P}$ and $R_{\rm AP}$ versus the temperature under different $\boldsymbol{K}_{\rm h}\cdot\alpha_0 = \pi/6$, $\pi/3$, and $\pi/2$, (d) $v(\boldsymbol{K}_{\rm h})$ versus $\boldsymbol{K}_{\rm h}\cdot\alpha_0$ at 300 K, where $\sigma = 0.08$, $T_{\rm C} = 800$ K, and $d = 1.5$ nm.

First, we would like to study the effect of the strain. The results are depicted in Fig. 3, where $\boldsymbol{K}_{\rm h}\cdot\alpha_0$ varies from $\pi/6$ to $\pi/2$, $\sigma = 0.08$, $T_{\rm C} = 800$ K, and $d = 1.5$ nm. Figure 3(a) shows the dependences of $R_{\rm P}$ and $R_{\rm AP}$ on the strain when $T = 300$ K. It can be found that both the $R_{\rm P}$ and $R_{\rm AP}$ increase with the strain, which is quite different from the oscillating phenomenon in MTJs with normal electrodes. For $R_{\rm AP}$, this is because it decreases with $v(\boldsymbol{K}_{\rm h})$ and also $v(\boldsymbol{K}_{\rm h})$ decreases with $\boldsymbol{K}_{\rm h}\cdot\alpha_0$ monotonously as shown in Figs. 2 and 3(d). For $R_{\rm P}$, this is because, in the present case, $v(\boldsymbol{K}_{\rm h})$ decreases more slowly when compared to the MTJs with normal electrodes. Therefore, $R_{\rm P}$ only varies within the increasing region. Interestingly, TMR oscillates with the strain which can be seen in Fig. 3(b). This originates from the oscillating behavior of $R_{\rm P}$ on $v(\boldsymbol{K}_{\rm h})$, and is in agreement with the experiments.[16–18] As shown in Fig. 3(b), the TMR can change about 30% by varying the strain. In addition, the temperature dependences of $R_{\rm P}$ and $R_{\rm AP}$ under different strain are also studied, which are shown in Fig. 3(c). It can be seen that $R_{\rm P}$ oscillates with the temperature whereas $R_{\rm AP}$ monotonously decreases with it. This can be understood from Eq. (5) that $v(\boldsymbol{K}_{\rm h})$ is a monotone increasing function of temperature. From Fig. 3(c), it can also be seen that both $R_{\rm P}$ and $R_{\rm AP}$ become more sensitive to temperature when the strain becomes larger. This can also be understood from Eq. (5) that $v(\boldsymbol{K}_{\rm h})$ will be more sensitive to temperature if a larger strain is applied.

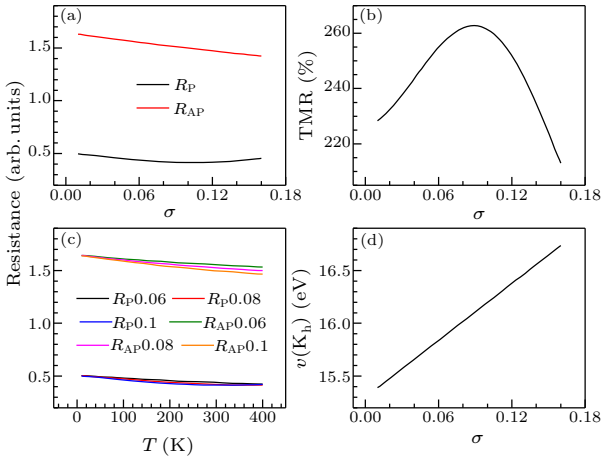

Fig. 4. (a) $R_{\rm P}$ and $R_{\rm AP}$ versus σ at 300 K, (b) TMR versus σ at 300 K, (c) $R_{\rm P}$ and $R_{\rm AP}$ versus the temperature under different $\sigma = 0.06$, 0.08, and 0.1, (d) $v(\boldsymbol{K}_{\rm h})$ versus σ at 300 K, where $\boldsymbol{K}_{\rm h}\cdot\alpha_0 = \pi/3$, $T_{\rm C} = 800$ K, and $d = 1.5$ nm.

Second, we investigate the effect of the defect concentration. The results are depicted in Fig. 4, where σ varies from 0.01 to 0.16, $\boldsymbol{K}_{\rm h}\cdot\alpha_0 = \pi/3$, $T_{\rm C} = 800$ K, and $d = 1.5$ nm. Figure 3(a) shows the dependences of $R_{\rm P}$ and $R_{\rm AP}$ on the defect concentration when $T = 300$ K. It can be found that $R_{\rm AP}$ decreases with σ whereas $R_{\rm P}$ oscillates with σ. For $R_{\rm AP}$, this is because it decreases with $v(\boldsymbol{K}_{\rm h})$ and $v(\boldsymbol{K}_{\rm h})$ increases with σ monotonously. For $R_{\rm P}$, this is because the $v(\boldsymbol{K}_{\rm h})$ varies more strongly with σ than with the strain, as can be seen in Fig. 4(d). In such a wide range of $v(\boldsymbol{K}_{\rm h})$, the oscillating behavior of $R_{\rm P}$ on $v(\boldsymbol{K}_{\rm h})$ will exhibit. Combining the results of $R_{\rm P}$ and $R_{\rm AP}$, the TMR will oscillate with σ, which can be seen in

Fig. 4(b). Due to the strong influence of defect concentration on $v(\boldsymbol{K}_{\rm h})$, the TMR can change about 50% by varying the defect concentration. In addition, the temperature dependences of $R_{\rm P}$ and $R_{\rm AP}$ under different defect concentrations are also studied, which are shown in Fig. 4(c). It can be seen that both the $R_{\rm P}$ and $R_{\rm AP}$ monotonously decreases with the temperature. The behavior of $R_{\rm AP}$ can be easily understood. For $R_{\rm P}$, it should oscillate with the temperature as stated above. However, in the present case, $R_{\rm P}$ only varies within the decreasing region of the whole oscillating period. From Fig. 4(c), it can also be seen that both $R_{\rm P}$ and $R_{\rm AP}$ are not sensitive to temperature. This can also be understood from Eq. (5) that $v(\boldsymbol{K}_{\rm h})$ will be not sensitive to temperature if both the defect concentration and the strain are not high.

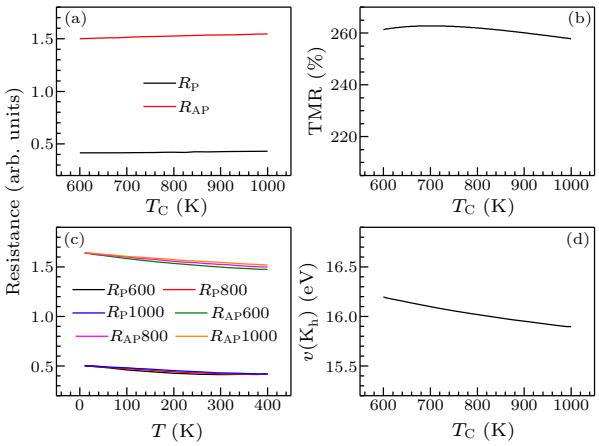

Fig. 5. (a) $R_{\rm P}$ and $R_{\rm AP}$ versus $T_{\rm C}$ at 300 K, (b) TMR versus $T_{\rm C}$ at 300 K, (c) $R_{\rm P}$ and $R_{\rm AP}$ versus the temperature under different $T_{\rm C} = 600$ K, 800 K, and 1000 K, (d) $v(\boldsymbol{K}_{\rm h})$ versus $T_{\rm C}$ at 300 K, where $\boldsymbol{K}_{\rm h}\cdot\alpha_0 = \pi/3$, $\sigma = 0.08$, and $d = 1.5$ nm.

Finally, we discuss the effect of the recovery temperature. The results are depicted in Fig. 5, where $T_{\rm C}$ varies from 600 K to 1000 K, $\boldsymbol{K}_{\rm h}\cdot\alpha_0 = \pi/3$, $\sigma = 0.08$, and $d = 1.5$ nm. Figure 5(a) shows the dependences of $R_{\rm P}$ and $R_{\rm AP}$ on the recovery temperature when $T = 300$ K. It can be found that both the $R_{\rm P}$ and $R_{\rm AP}$ quite slowly increases with $T_{\rm C}$. This happens because the $v(\boldsymbol{K}_{\rm h})$ varies little with $T_{\rm C}$ at present, as can be seen in Fig. 5(d). As a natural result, the TMR oscillates with $T_{\rm C}$ but the amplitude is less than 10%, which can be seen in Fig. 5(b). In addition, the temperature dependences of $R_{\rm P}$ and $R_{\rm AP}$ under different recovery temperatures are also studied, which are shown in Fig. 5(c). The situation and discussion are analogous to Fig. 4(c).

In summary, we have developed a tunneling theory to study the effect of lattice distortion on the MTJs consisting of single-crystal barrier and half-metallic electrodes. In the present theory, the energy of the tunneling electron can be non-conserved, and therefore, TMR can be finite if $v(\boldsymbol{K}_{\rm h}) > \Delta - \mu$ even both the electrodes are half-metallic. Meanwhile, the lattice distortion is described by three physical parameters, i.e., strain, defect concentration and recovery temperature. All the three parameters will modify the periodic scattering potential, and further alter $R_{\rm P}$ and $R_{\rm AP}$. Finally, we have discussed respectively the effect of the three parameters on the MTJs. It is found that: (1) The TMR oscillates with all the three parameters. (2) The strain can change the TMR about 30%. (3) The defect concentration will strongly modify the periodic scattering potential, and further change the TMR about 50%. (4) The recovery temperature has little effect on the periodic scattering potential, and only can change the TMR about 10%. Among the three parameters of the strain, defect concentration and recovery temperature, the effect of defect concentration is the strongest, while that of recovery temperature is the weakest. These results may possess theoretical guidance to the further research and applications for the MTJs consisting of single-crystal barrier and half-metallic electrodes.

References

[1] Han X F, Oogane M, Kubota H et al 2000 *Appl. Phys. Lett.* **77** 283
[2] Parkin S S P, Kaiser C, Panchula A et al 2004 *Nat. Mater.* **3** 862
[3] Yuasa S, Nagahama T, Fukushima A et al 2004 *Nat. Mater.* **3** 868
[4] Drewello V, Schmalhorst J, Thomas A et al 2008 *Phys. Rev. B* **77** 014440
[5] Fuchs G D, Katine J A, Kiselev S I et al 2006 *Phys. Rev. Lett.* **96** 186603
[6] Kubota H, Fukushima A, Yakushiji K et al 2008 *Nat. Phys.* **4** 37
[7] Deac A M, Fukushima A, Kubota H et al 2008 *Nat. Phys.* **4** 803
[8] Jia X T, Xia K and Bauer G E W 2011 *Phys. Rev. Lett.* **107** 176603
[9] Fabian J, Matos-Abiaguea A, Ertlera C et al 2007 *Acta Phys. Slovaca* **57** 565
[10] Han X F, Ali S S and Liang S H 2013 *Sci. Chin. Phys. Mech.* **56** 29
[11] Ishikawa T, Hakamata S, Matsuda K et al 2008 *J. Appl. Phys.* **103** 07A919
[12] Hu B, Moges K, Honda Y et al 2016 *Phys. Rev. B* **94** 094428
[13] Liu H, Kawami T, Moges K et al 2015 *J. Phys. D* **48** 164001
[14] Marukame T, Ishikawa T, Taira T et al 2010 *Phys. Rev. B* **81** 134432
[15] Zhang J, Phung T, Pushp A et al 2017 *Appl. Phys. Lett.* **110** 172403
[16] McFadden A, Wilson N, Brown-Heft et al 2017 *J. Magn. Magn. Mater.* **444** 383
[17] McFadden A, Brown-Heft, Pennachio D et al 2017 *J. Appl. Phys.* **122** 113902
[18] Inoue M, Hu B, Moges K et al 2017 *Appl. Phys. Lett.* **111** 082403
[19] Fang H N, Xiao M W, Rui W B et al 2018 *J. Magn. Magn. Mater.* **465** 333
[20] Fang H N, Xiao M W, Rui W B et al 2016 *Sci. Rep.* **6** 24300
[21] Cowley J M 1995 *Diffraction Physics* (Amsterdam: Elsevier)
[22] Fang H N, Xiao M W, Rui W B et al 2019 *New J. Phys.* **21** 123006